Expression of ovarian tumour suppressor OPCML in the female CD-1 mouse reproductive tract

Jean S Fleming[1], **H James McQuillan**[1], **Melanie J Millier**[1], and **Grant C Sellar**[2]

[1]Department of Anatomy and Structural Biology, University of Otago School of Medical Sciences, PO Box 913, Dunedin, New Zealand 9054

[2]University of Edinburgh and Cancer Research UK Cancer Research Centre, University of Edinburgh, Crewe Road South, Edinburgh EH4 2XR, UK*

Abstract

Opioid binding protein/cell adhesion molecule-like gene (OPCML) is frequently inactivated in epithelial ovarian cancer, but the role of this membrane protein in normal reproductive function is unclear. The ovarian surface epithelium (OSE) is thought to be the cell of origin of most epithelial ovarian cancers, some of which arise after transformation of OSE cells lining ovarian inclusion cysts, formed during ovulation. We used immunohistochemistry immunoblotting and quantitative RT-PCR (qRT-PCR) to investigate OPCML expression in the uteri and ovaries of cycling 3-month CD-1 mice, as well as in ovaries from older mice containing inclusion cysts derived from rete ovarii tubules. Immunoblotting showed OPCML bands in uterine, but not whole ovarian or muscle extracts. Strong OPCML immunoreactivity was observed in oviduct, rete ovarii and uterus, whereas in ovary more immunoreactivity was seen in granulosa cells than OSE. No staining was observed in OSE around ovulation sites, where OSE cells divide to cover the site. OPCML immunoreactivity was also weaker in more dysplastic cells lining large ovarian inclusion cysts, compared with normal rete ovarii. No significant changes in OPCML mRNA expression were observed in whole ovarian and uterine extracts at different stages of the cycle. We conclude murine OPCML is more consistently expressed in cells lining the uterus, oviduct and rete ovarii than in ovary and is not expressed in OSE associated with ovulation sites. This observation supports the hypothesis that a proportion of epithelial ovarian cancers arise from ductal cells and other epithelia of the secondary Mullerian system, rather than the OSE.

Keywords

IgLON; opioid binding protein/cell adhesion molecule-like gene

---

Correspondence, Professor Jean. S. Fleming, Department of Anatomy & Structural Biology, University of Otago School of Medical Sciences, PO Box 913, Dunedin, New Zealand 9054, **Telephone**: +643 479 7848, **Fax**: +643 479 7254, **Email**: jean.fleming@otago.ac.nz.
*Current address: Wyeth Research and Translational Medicine Research Collaboration, TMRC Laboratory, Dundee DD1 9SY, UK.

Introduction

Opioid binding protein/cell adhesion molecule-like gene (OPCML) has been identified as a tumour suppressor protein that is frequently inactivated by allele loss and CpG island promoter methylation in ovarian and lung adenocarcinoma (Sellar *et al.* 2003; Tsou *et al.* 2007). OPCML, also called opioid binding cell adhesion molecule (OBCAM), was originally isolated from brain (Schofield *et al.* 1989), but has also been shown to be expressed in other tissues, including human stomach (Wang *et al.* 1989), whole ovary (Ntougkos *et al.* 2005; Teodoridis *et al.* 2005; Czekierdowski *et al.* 2006; Chen *et al.* 2007) and ovarian surface epithelium (OSE) (Sellar *et al.* 2003; Mei *et al.* 2006), but not in rat kidney or liver (Hachisuka *et al.* 1996). OPCML belongs to the IgLON (LSAMP, OPCML/ OBCAM, neurotrimin) family of immunoglobulin (Ig) domain-containing glycosylphosphatidylinositol (GPI)-anchored cell adhesion molecules (Lodge *et al.* 2000; Miyata *et al.* 2003a; Miyata *et al.* 2003b; Reed *et al.* 2004; Ntougkos *et al.* 2005). *In vivo*, epithelial ovarian cancers show reduced *OPCML* expression as the result of epigenetic inactivation or mutation (Sellar *et al.* 2003; Ntougkos *et al.* 2005). Conversely, transfection of epithelial ovarian cancer cell lines *in vitro* with sense *OPCML* transcripts results in reduced rates of culture growth, relative to the parent cell line (Sellar *et al.* 2003) or to transfected normal CD1 mouse ovarian surface epithelial cells (Yao *et al.* 2006), suggesting OPCML functions to control cell proliferation and tumour size. The rodent *Opcml* cDNA shows >90% identity and the protein >98% identity to the human sequences, implying conservation of function between these species (Shark and Lee 1995). However the role of this protein in normal ovarian tissue remains to be described.

We have examined *Opcml* mRNA and protein expression in the mouse ovary and uterus, using quantitative real-time reverse transcription PCR (qRT-PCR), immunoblotting and immunohistochemistry, with the aim of characterizing expression of OPCML in the normal female mouse reproductive system. We hypothesised that OPCML expression would be reduced in cells undergoing cell division, for example, in the OSE at the edges of recent ovulation sites (Tan and Fleming 2004). Our previous studies demonstrated that ovaries of CD-1 out-bred mice subjected to incessant ovulation (IO) showed an increased number of surface invaginations, stratification of the OSE, cortical inclusion cyst formation and dilation of the rete ovarii tubules, similar to preneoplastic changes in the human ovary (Fleming *et al.* 2006; Fleming *et al.* 2007). We have therefore investigated OPCML protein immunoreactivity in the cystic ovaries of CD-1 mice subjected to incessant ovulation and containing large cystic structures, likely to be dilated rete ovarii tubules (Tan *et al.* 2005), to determine if OPCML expression changes in these cystic structures. As far as we are aware, this is the first report on the localisation of expression of OPCML in the mammalian reproductive system to date.

Materials and Methods

Animals

The University of Otago Animal Ethics Committee approved all experiments. Female out-bred CD-1 (Swiss Webster) mice were housed post-weaning in a temperature- and light-controlled facility with 12 hours light and 12 hours darkness. Mice were held in cages divided by a screen, alongside a male, to induce continuous ovulation cycles, as previously described (Clow *et al.* 2002; Tan and Fleming 2004). Stage of oestrous cycle was determined by vaginal cytology before 10.00 am, using the lavage method, until regular cycles were detected (Blaustein 1981; Clow *et al.* 2002). Animals (3-4 months old) were euthanized with halothane gas and exsanguination on the days of proestrus (n=5), oestrous (n=5), dioestrus (n=3) or metoestrus (n=4). One ovary and samples of uterus were fixed overnight in 4% paraformaldehyde for immunohistochemistry, as described (Fleming *et al.*

2007). Ovarian and whole uterine horn samples were also frozen in liquid nitrogen and stored at -80 °C for RNA analysis.

Induction of ovarian inclusion cysts with age and incessant ovulation

CD-1 mice were housed beside, but not in contact with a male in a divided cage, to induce incessant ovulation (IO group) and prevent breeding, as previously described (Fleming *et al.* 2007), from age of weaning until 6, 9 or 12-months of age. All animals were euthanized and dissected on the afternoon of oestrus (Fleming *et al.* 2007).

Immunoblotting

A chicken anti-human OPCML monoclonal antibody was used for immunoblot and immunohistochemical analysis (Sellar *et al.* 2003). Samples of mouse whole ovary, uterus and skeletal muscle (negative control) were snap frozen, pulverized in liquid nitrogen and the protein extracted as previously described (Fleming *et al.* 2007). Protein concentrations were determined using a bicinchoninic acid protein assay kit (Pierce Biotechnology, Rockford, IL). Protein extracts (5 and 20 µg protein) were separated on discontinuous 10% SDS-PAGE gels and electroblotted onto polyvinylidene difluoride membranes (PVDF, Roche Pharmaceuticals, Auckland, New Zealand). A 10-250 KDa pre-stained protein marker was loaded onto all gels. Blots were incubated with 10% skim milk powder in phosphate buffered saline, pH 7.4 (PBS) plus 0.1% Tween 20, for 1 hour at room temperature to reduce non-specific binding, then probed for 1 h at room temperature with a 1:4000 dilution of OPCML primary antibody (Sellar *et al.* 2003) in PBS containing 0.1% (v/v) Tween 20 and 3% (w/v) skim milk powder (PBS-TM). Membranes were washed and incubated with horseradish-peroxidase-conjugated anti-chicken secondary antibody (Amersham Pharmacia Biotech UK; diluted 1:2000 in PBS-TM) for 1 h at room temperature, prior to detection of bound antibody with the ECL chemiluminescent detection system (Amersham Pharmacia Biotech UK) according to the manufacturer's directions.

Immunohistochemistry

Serial sections (4 µm) were cut from each ovary and 10-20 sections cut from uterine samples, dewaxed and rehydrated as described (Fleming, McQuillan *et al.* 2007). Up to 10 sections were stained per tissue sample. Antigen retrieval was performed by boiling in a 700-watt microwave for 10 minutes in 0.01 M citrate buffer (pH 6.0). Slides were left to stand for 15 minutes in hot buffer before being washed in PBS. Endogenous peroxidase was blocked with 3% hydrogen peroxide in methanol for 5 minutes and, after further washes in PBS plus 1% (v/v) Triton X-100, non-specific binding was minimized by blocking with avidin-biotin blocking reagents (Zymed Laboratories Inc., San Francisco, CA, USA) and 20% (v/v) normal goat serum (Sigma-Aldrich Inc. USA, 1:20 in PBS, 30 minutes). Sections were incubated overnight at 4°C with a 1:30 dilution of primary antibody, followed by incubation in biotinylated goat anti-chicken secondary antibody for 30 minutes (Amersham Pharmacia Biotech UK, 1/200) in PBS). Further washing in PBS plus 1% (v/v) Triton X-100 was followed by incubation in streptavidin biotinylated horseradish peroxidase for 30 minutes (Amersham Pharmacia Biotech UK, 1/100) in PBS. Antibody complex was detected with diaminobenzidine (DAB; Vector Laboratories Inc. Peterborough, UK). Sections were counter-stained with Gills haematoxylin.

OPCML immunoreactivity was examined in 70 stained 4 µm sections from 20 CD-1 mice (3 or 6 months, in oestrus). The intensity of the immunoreactive staining in a range of cellular compartments in the stained ovarian sections was graded on a range of 0-3, where 0 was negative, 1 was mild, cytoplasmic staining and 3 indicated strong, membrane-situated OPCML immunoreactivity.

RNA extraction

Total RNA was extracted from frozen whole ovaries and uteri (30 ± 6 μg tissue), using the Qiagen RNeasy Mini Kit according to manufacturer's directions (Qiagen Pty. Ltd., Victoria, Australia). RNA concentration and quality were determined by spectrophotometry in an ND-1000 Nanodrop UV/Vis spectrophotometer (Nanodrop Technologies, Wilmington, DE, USA). Samples were diluted 1:10 in RNase-free water for concentration measurements and in 10 mM Tris HCl, pH 7.5, for purity measurements. RNA quality was also assessed by electrophoresis of 1 μg each sample through a 1% non-denaturing agarose gel (data not shown). Samples showing signs of RNA degradation were not assessed for *Opcml* mRNA expression by qRT-PCR.

Reverse transcription and semi-quantitative PCR

Total RNA (1-2 μg) was reverse transcribed using Superscript III reverse transcriptase (Invitrogen, USA) and 200 ng random primers (Invitrogen, USA) in a total volume of 20 μL, at 50°C for 60 min and at 70°C for15 min. A stock of reference cDNA for qRT-PCR was obtained by reverse transcribing 5 μg total RNA from mouse uterus using random hexamers. A serial dilution of this stock cDNA was used to estimate relative *Opcml* and endogenous β-actin mRNA concentrations for both ovarian and uterine samples. Primers and FAM-labelled probes for Taqman qRT-PCR of mouse *Opcml* and β-actin sequences were obtained from Applied Biosystems Assays-on-Demand (Applied Biosystems Mm00625983 m1 and 4352933E corresponding to NM 177906 and NM 007393.1, respectively). The *Opcml* probes amplified sequence between exons 3 and 4 of the mouse *Opcml* gene (http://www.ncbi.nlm.nih.gov/genome/probe/reports/).

Opcml mRNA concentration was then normalized relative to the concentration of endogenous β-actin mRNA. *Opcml* and β-actin cDNA were amplified in the same Taqman run. The mean (± sd) correlation coefficient (R^2) for standard curves was 0.994 ± 0.005. Samples for qRT-PCR analysis were run in duplicate in 20 μl reaction volumes with 300 nM target-specific primers and 200 nM fluorescent probe, using the Taqman Universal PCR mix in an ABI Prism 7000 quantitative gene amplification system (Applied Biosystems, Foster City, CA, USA). Controls without RT were included in each run to assess the contribution of genomic DNA in the reactions (not detectable; data not shown).

Results

OPCML immunoblot

The chicken anti-human OPCML monoclonal antibody showed Opcml immunoreactive bands on western blots of uterine protein extracts, but not in whole ovarian or muscle extracts. Two bands at approximately 42 and 50 KDa were observed (Figure 1), similar to results previously reported in rat brain (Miyata *et al*. 2000; Yamada *et al*. 2007).

OPCML immunohistochemistry

Strong membrane staining in the luminal epithelium and endometrial glands of mouse uterus was observed by immunohistochemistry with the chicken anti-human OPCML antibody (Figure 2a). In addition, strong staining was seen in the oviduct epithelium (Figure 2e and f) and on the luminal surfaces of cells lining the rete ovarii (Figures 2d and 3a). Immunostaining intensity in the different ovarian cellular compartments was graded in 3- or 6-month mice at oestrus. Average ± sd staining intensities are shown in Table 1. The mouse ovarian surface epithelium (OSE) showed patchy immunoreactivity, with parts of the OSE positively stained and other parts remaining unstained (Figures 2b, 2c and 3c). All ovaries examined had areas of positive OPCML immunoreactivity in the OSE. More consistent staining was seen in the cytoplasm of granulosa cells of healthy and atretic antral ovarian

follicles (Table 1; Figures 2b, 2c and 3c), especially in fresh ovulation sites, whereas the OSE associated with fresh ovulation sites was negative (Figure 2c). The granulosa cells of primordial and primary follicles were rarely immuno-positive for OPCML (Table 1). The zona pellucida of oocytes stained in some, but not all small and antral follicles (Table 1; Figures 2b and 3c).

OPCML immunoreactive staining was observed in cells lining normal (Figure 2d) and dilated rete ovarii in the ovaries of 9-month and 12-month old mice subjected to incessant ovulation (Figures 3a, 3c and 3e). Flattened or ciliated cells and columnar secretory cells lining cystic rete ovarii tubules showed less reactivity compared with signet ring cells, with no clear membrane delineation of the immunoreactivity (Figures 3c-f). OSE stained noticeably weaker than cyst epithelium in some sections (Figure 3c). Stronger OPCML staining was seen on the cells lining the one cortical inclusion cyst observed in this study (Figure 3b), primarily on the basal surface of the luminal cell layer.

Quantitative RT-PCR

No difference in the average yield of total RNA (mean ± sd) between ovarian and uterine samples was observed ($17 \pm 10 \, \mu g$ RNA), and samples had an average OD_{260}:OD_{280} ratio (mean ± sd) of 1.93 ± 0.16. Higher expression of *Opcml* (relative to β-actin) was measured in mouse uterus than whole ovary, but no significant differences in relative *Opcml* expression were observed in either tissue across the stages of the oestrous cycle (Table 2). There was considerable inter-animal variation in the relative amounts of *Opcml* expression measured in whole extracts of both tissues.

Discussion

OPCML is a member of the IgLON family of opioid-binding cell adhesion molecules (including limbic system-associated membrane protein (LSAMP), neuronal growth regulator 1 (NEGR1/Kilon) and neurotrimin), which form homo- or hetero-dimeric DigLONs that affect cell adhesion and cell signalling (Reed *et al.* 2004; Reed *et al.* 2007). The Iglons are most highly expressed in brain and other neural tissue, largely in dendritic membranes, and may modify dendrite growth (Reed *et al.* 2007). Loss of *OPCML* mRNA has been reported in sporadic epithelial ovarian cancer (Sellar *et al.* 2003; Ntougkos *et al.* 2005), gastric cancer (Wang *et al.* 2006), gliomas and other brain tumours (Reed *et al.* 2007) using either qRT-PCR or microarray. The current study of OPCML expression is the first to detail the localisation of immunoreactivity of this protein in the female mammalian reproductive system.

More OPCML expression was detected in uterus than in ovary using a variety of techniques. Expression of OPCML protein has been observed (GC Sellar, unpublished data), but not been reported previously in uterus. We could detect no significant changes in expression through the oestrous cycle, in extracts of whole uterine horn, despite strong epithelial immunoreactivity. When the *Symatlas* database (http://symatlas.gnf.org/SymAtlas/) was used to determine the relative expression of *Opcml* in a variety of tissues *in silico*, low average levels of expression were recorded for most tissues, including ovary and uterus, in comparison with neural tissues, for both human and mouse. Given the proliferative changes shown in the uterus throughout the cycle, the lack of variation with cycle is surprising, but may have been a result of once a day sampling of tissues. A more detailed study on the expression of OPCML in uterine epithelia and in endometrial carcinoma is warranted. Although two *OPCML* splice variants, alpha1 and alpha2, have been identified recently in humans (Reed *et al.* 2007), the primers used to amplify *Opcml* in ovary and uterus would not have distinguished between the variants.

Immunoblotting with a chicken anti-human OPCML monoclonal antibody showed two bands at approximately 42 and 50 KDa, in mouse uterine extracts, but not in ovary or skeletal muscle. The size of the murine OPCML protein has been reported as 58 and 51 KDa in membrane preparations of bovine, rat, mouse, guinea pig and rabbit brains (Hachisuka *et al.* 1996). Two immunoreactive bands of 46 and 51 KDa have also been reported for rat OPCML protein (Miyata *et al.* 2000). These are thought to be isoforms that differ in the amount or type of glycosylation (Yamada *et al.* 2007). The lack of immunoreactivity on immunoblots of whole ovarian extracts suggests low concentrations of OPCML protein are expressed or that expression of the protein is confined to a small number of specific cells in this tissue. Alternatively, the protein extraction methods may decrease epitope availability for the antibody used.

The immunoblotting results contrast with those obtained by immunohistochemistry, in both mouse and human tissues, with the same antibody (Sellar *et al.* 2003). OPCML immunoreactivity was detected inconsistently in mouse OSE by immunohistochemistry, despite staining in granulosa cells of larger follicles, particularly around ovulation sites. The granulosa cell immunostaining appeared not to be membrane delineated, compared with the strong immunoreactivity in uterus, oviduct and rete ovarii tubules. No OPCML immunoreactivity was observed in the OSE at the edges of fresh ovulation sites (Figure 2c). This is consistent with the protein having a role in the suppression of cell proliferation (Sellar *et al.* 2003; Ntougkos *et al.* 2005; Reed *et al.* 2007; Cui *et al.* 2008), since cell division is frequently observed in the OSE at the base of ovulation sites (Tan and Fleming 2004).

Normal extra-ovarian rete ovarii tubules showed strong membrane-limited OPCML immunostaining and this immunoreactivity decreased as the rete ovarii tubules dilated and formed cysts, again consistent with the hypothesis that OPCML expression decreases in dividing cells. The more dysplastic cells in cysts showed the least staining, suggesting a loss of epitope. Whilst this mouse model of ovarian inclusion cyst formation does not produce ovarian tumours (Fleming *et al.* 2007), the changes in OPCML immunoreactivity observed during cyst formation parallel those observed during human epithelial ovarian carcinogenesis (Sellar *et al.* 2003). These results contrast with those observed for E-cadherin, where ciliated, cuboidal cyst cells maintained strong immunoreactivity (Fleming *et al.* 2007).

The epithelia of the fimbria and distal fallopian tube have been implicated recently in serous epithelial ovarian carcinogenesis, particularly in carriers of BRCA1 mutations (Medeiros *et al.* 2006; Callahan *et al.* 2007; Crum *et al.* 2007; Kindelberger *et al.* 2007; Jarboe *et al.* 2008). The observation of strong OPCML immunoreactivity in the mouse oviduct, but not the OSE, supports the hypothesis that a proportion of epithelial ovarian cancers arise from ductal cells. We conclude from this initial study that a decrease in OPCML expression is associated with sites of increased cell division in the normal and cystic CD-1 mouse ovary. The results obtained in extracts from whole mouse ovary and uterus and the presence of OPCML immunoreactivity in uterine epithelia and granulosa cells suggest further studies of this important tumour suppressor at a cellular, rather than whole tissue level are warranted.

Acknowledgments

References

Blaustein A. Surface (germinal) epithelium and related ovarian neoplasms. Pathology Annual. 1981; 16:247–94. [PubMed: 7329732]

Callahan MJ, Crum CP, Medeiros F, Kindelberger DW, Elvin JA, Garber JE, Feltmate CM, Berkowitz RS, Muto MG. Primary fallopian tube malignancies in BRCA-positive women undergoing surgery for ovarian cancer risk reduction. Journal of Clinical Oncology. 2007; 25:3985–90. [PubMed: 17761984]

Chen H, Ye F, Zhang J, Lu W, Cheng Q, Xie X. Loss of OPCML expression and the correlation with CpG island methylation and LOH in ovarian serous carcinoma. European Journal of Gynaecological Oncology. 2007; 28:464–7. [PubMed: 18179137]

Clow OL, Hurst PR, Fleming JS. Changes in the mouse ovarian surface epithelium with age and ovulation number. Molecular and Cellular Endocrinology. 2002; 191:105–11. [PubMed: 12044924]

Crum CP, Drapkin R, Kindelberger D, Medeiros F, Miron A, Lee Y. Lessons from BRCA: the tubal fimbria emerges as an origin for pelvic serous cancer. Clinical Medicine & Research. 2007; 5:35–44. [PubMed: 17456833]

Cui Y, Ying Y, van Hasselt A, Ng KM, Yu J, Zhang Q, Jin J, Liu D, Rhim JS, Rha SY, Loyo M, Chan AT, Srivastava G, Tsao GS, Sellar GC, Sung JJ, Sidransky D, Tao Q. OPCML is a broad tumor suppressor for multiple carcinomas and lymphomas with frequently epigenetic inactivation. PLoS ONE. 2008; 3:e2990. [PubMed: 18714356]

Czekierdowski A, Czekierdowska S, Szymanski M, Wielgos M, Kaminski P, Kotarski J. Opioid-binding protein/cell adhesion molecule-like (OPCML) gene and promoter methylation status in women with ovarian cancer. Neuro Endocrinology Letters. 2006; 27:609–13. [PubMed: 17159813]

Fleming JS, Beaugie CR, Haviv I, Chenevix-Trench G, Tan OL. Incessant ovulation, inflammation and epithelial ovarian carcinogenesis: revisiting old hypotheses. Molecular & Cellular Endocrinology. 2006; 247:4–21. [PubMed: 16297528]

Fleming JS, McQuillan HJ, Millier MJ, Beaugie CR, Livingstone V. E-cadherin expression and bromodeoxyuridine incorporation during development of ovarian inclusion cysts in age-matched breeder and incessantly ovulated CD-1 mice. Reproductive Biology & Endocrinology. 2007; 5:14. [PubMed: 17425809]

Hachisuka A, Yamazaki T, Sawada J, Terao T. Characterization and tissue distribution of opioid-binding cell adhesion molecule (OBCAM) using monoclonal antibodies. Neurochemistry International. 1996; 28:373–9. [PubMed: 8740443]

Jarboe E, Folkins A, Nucci MR, Kindelberger D, Drapkin R, Miron A, Lee Y, Crum CP. Serous carcinogenesis in the fallopian tube: a descriptive classification. International Journal of Gynecological Pathology. 2008; 27:1–9. [PubMed: 18156967]

Jo M, Gieske MC, Payne CE, Wheeler-Price SE, Gieske JB, Ignatius IV, Curry TE Jr, Ko CM. Development and application of a rat ovarian gene expression database. Endocrinology. 2004; 145:5384–96. [PubMed: 15297439]

Kindelberger DW, Lee Y, Miron A, Hirsch MS, Feltmate C, Medeiros F, Callahan MJ, Garner EO, Gordon RW, Birch C, et al. Intraepithelial carcinoma of the fimbria and pelvic serous carcinoma: Evidence for a causal relationship. Americam Journal of Surgical Pathology. 2007; 31:161–9.

Lodge AP, Howard MR, McNamee CJ, Moss DJ. Co-localisation, heterophilic interactions and regulated expression of IgLON family proteins in the chick nervous system. Molecular Brain Research. 2000; 82:84–94. [PubMed: 11042360]

Medeiros F, Muto MG, Lee Y, Elvin JA, Callahan MJ, Feltmate C, Garber JE, Cramer DW, Crum CP. The tubal fimbria is a preferred site for early adenocarcinoma in women with familial ovarian cancer syndrome. American Journal Surgical Pathology. 2006; 30:230–6.

Mei FC, Young TW, Liu J, Cheng X. RAS-mediated epigenetic inactivation of OPCML in oncogenic transformation of human ovarian surface epithelial cells. Faseb Journal. 2006; 20:497–9. [PubMed: 16384911]

Miyata S, Funatsu N, Matsunaga W, Kiyohara T, Sokawa Y, Maekawa S. Expression of the IgLON cell adhesion molecules Kilon and OBCAM in hypothalamic magnocellular neurons. Journal of Comparative Neurology. 2000; 424:74–85. [PubMed: 10888740]

Miyata S, Matsumoto N, Maekawa S. Polarized targeting of IgLON cell adhesion molecule OBCAM to dendrites in cultured neurons. Brain Research. 2003a; 979:129–36. [PubMed: 12850579]

Miyata S, N Matsumoto N, Taguchi K, Akagi A, Iino T, Funatsu N, Maekawa S. Biochemical and ultrastructural analyses of IgLON cell adhesion molecules, Kilon and OBCAM in the rat brain. Neuroscience. 2003b; 117:645–58. [PubMed: 12617969]

Ntougkos E, Rush R, Scott D, Frankenberg T, Gabra H, Smyth JF, Sellar GC. The IgLON family in epithelial ovarian cancer: expression profiles and clinicopathologic correlates. Clinical Cancer Research. 2005; 11:5764–8. [PubMed: 16115914]

Reed J, McNamee C, Rackstraw S, Jenkins J, Moss D. Diglons are heterodimeric proteins composed of IgLON subunits, and Diglon-CO inhibits neurite outgrowth from cerebellar granule cells. Journal of Cell Science. 2004; 117:3961–73. [PubMed: 15265982]

Reed JE, Dunn JR, du Plessis DG, Shaw EJ, Reeves P, Gee AL, Warnke PC, Sellar GC, Moss DJ, Walker C. Expression of cellular adhesion molecule 'OPCML' is down-regulated in gliomas and other brain tumours. Neuropatholology & Applied Neurobiology. 2007; 33:77–85.

Schofield PR, McFarland KC, Hayflick JS, Wilcox JN, Cho TM, Roy S, Lee NM, Loh HH, Seeburg PH. Molecular characterization of a new immunoglobulin superfamily protein with potential roles in opioid binding and cell contact. The EMBO Journal. 1989; 8:489–95. [PubMed: 2721489]

Sellar GC, Watt KP, Rabiasz GJ, Stronach EA, Li L, Miller EP, Massie CE, Miller J, Contreras-Moreira B, Scott D, et al. OPCML at 11q25 is epigenetically inactivated and has tumor-suppressor function in epithelial ovarian cancer. Nature Genetics. 2003; 34:337–43. [PubMed: 12819783]

Shark KB, Lee NM. Cloning, sequencing and localization to chromosome 11 of a cDNA encoding a human opioid-binding cell adhesion molecule (OBCAM). Gene. 1995; 155:213–7. [PubMed: 7721093]

Tan OL, Fleming JS. Proliferating cell nuclear antigen immunoreactivity in the ovarian surface epithelium of mice of varying ages and total lifetime ovulation number following ovulation. Biology of Reproduction. 2004; 71:1501–1507. [PubMed: 15229142]

Tan OL, Hurst PR, Fleming JS. Location of inclusion cysts in mouse ovaries in relation to age, pregnancy and total ovulation number: implications for ovarian cancer? Journal of Pathology. 2005; 205:483–490. [PubMed: 15685692]

Teodoridis JM, Hall J, Marsh S, Kannall HD, Smyth C, Curto J, Siddiqui N, Gabra H, McLeod HL, Strathdee G, et al. CpG island methylation of DNA damage response genes in advanced ovarian cancer. Cancer Research. 2005; 65:8961–7. [PubMed: 16204069]

Tsou JA, Galler JS, Siegmund KD, Laird PW, Turla S, Cozen W, Hagen JA, Koss MN, Laird-Offringa IA. Identification of a panel of sensitive and specific DNA methylation markers for lung adenocarcinoma. Molecular Cancer. 2007; 6:70. [PubMed: 17967182]

Wang F, Li ZY, Chi ZQ, Zeng ZK, Zong GY. Active opioid binding protein from rat brain--a glycoprotein containing alpha-methyl-D-mannoside residues. Zhongguo Yao Li Xue Bao. 1989; 10:481–4. [PubMed: 2561932]

Wang L, Zhu JS, Song MQ, Chen GQ, Chen JL. Comparison of gene expression profiles between primary tumor and metastatic lesions in gastric cancer patients using laser microdissection and cDNA microarray. World Journal of Gastroenterology. 2006; 12:6949–6954. [PubMed: 17109515]

Yamada M, Hashimoto T, Hayashi N, Higuchi M, Murakami A, Nakashima T, Maekawa S, Miyata S. Synaptic adhesion molecule OBCAM; synaptogenesis and dynamic internalization. Brain Research. 2007; 1165:5–14. [PubMed: 17658490]

Yao DS, Li L, Garson K, Vanderhyden BC. *OPCML gene transferred by recombinant lentiviruses in vitro and its inhibition to ovarian cancer cells. Zhonghua Fu Chan Ke Za Zhi. 2006; 41:333–8. [PubMed: 16762191]
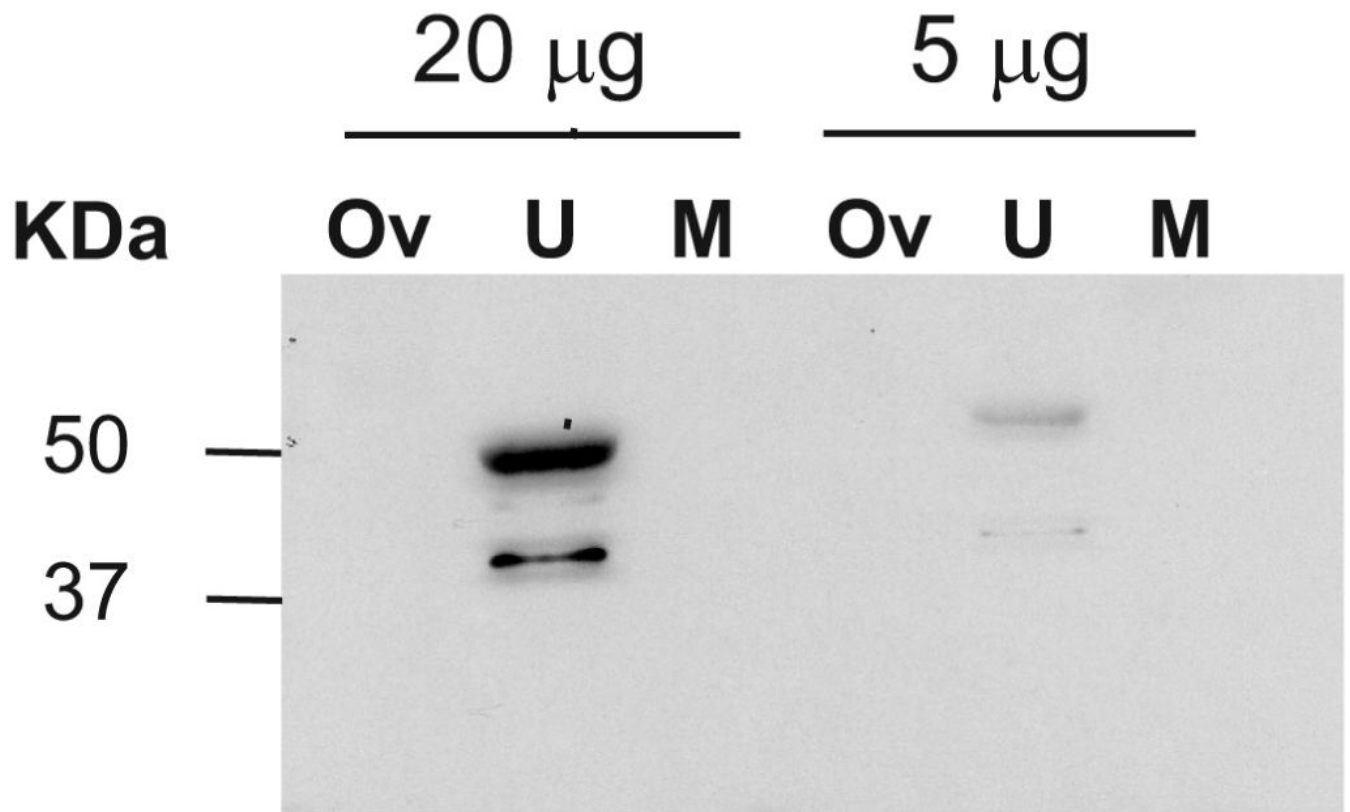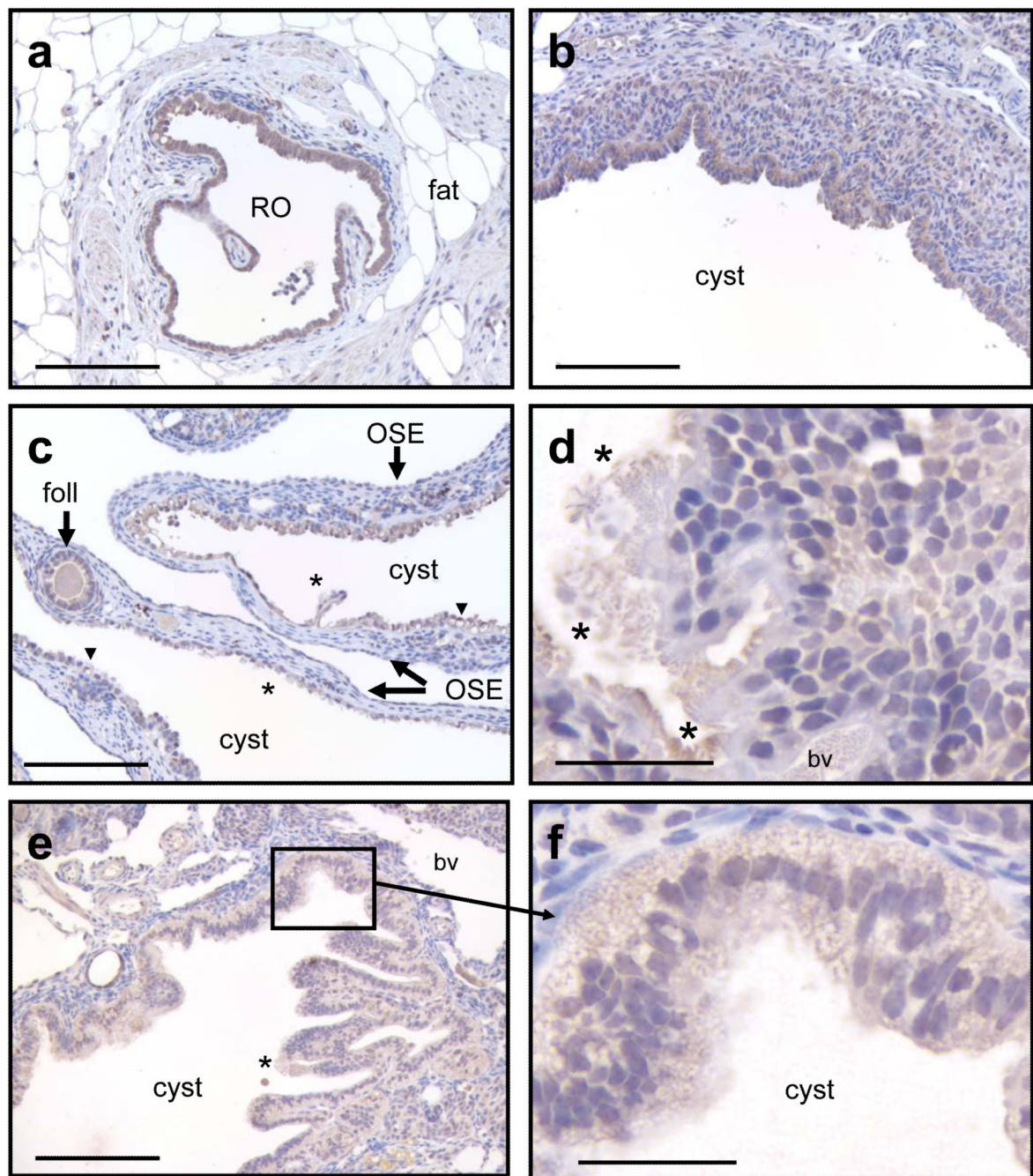
Figure 1.
Western blot of OPCML immunoreactivity in extracts of ovary (O), uterus (U) and skeletal muscle (M) from 3-month CD-1 mice. Two immunoreactive bands at approximately 42 KDa and 50 KDa were observed in uterine extracts only, even when 20-μg protein was loaded onto the polyacrylamide gel.
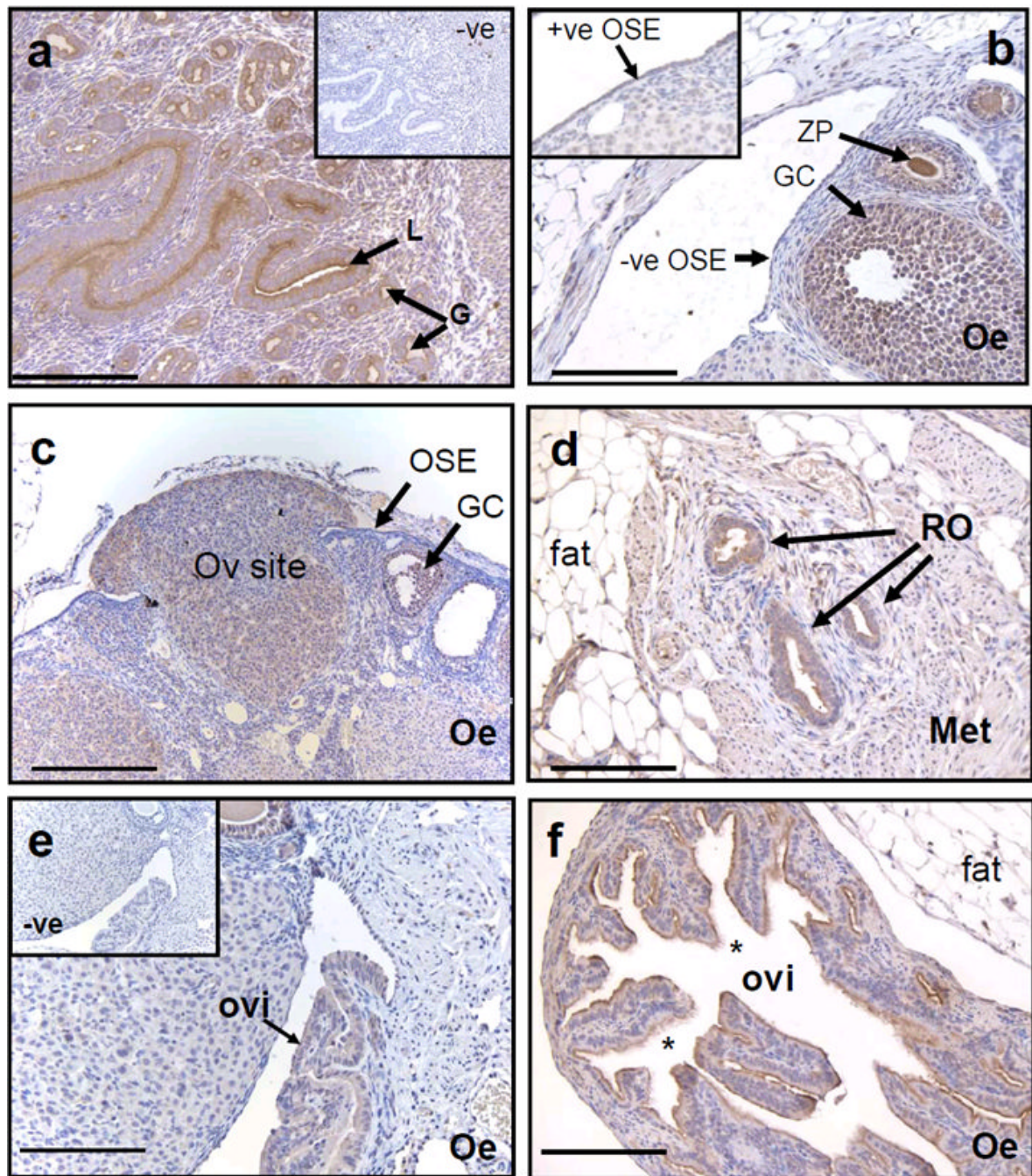
Figure 2.
OPCML immunohistochemistry in 4μm sections of CD-1 mouse uterus (a), ovaries (b-d) and oviducts (e and f) obtained in the morning of (b and c, e and f) oestrus (Oe) and (d) metoestrus (Met). A fresh ovulation site (Ov site) is seen in (c), with the granulosa cells spilling over and covering the OSE, which is immuno-negative in comparison with the granulosa cells of the ovulated follicle. Negative controls, without primary antibody, are shown in the insets of (a) and (e). The inset of (b) shows an example of positive OPCML immunoreactivity in the OSE. (a) OPCML staining was observed on the luminal surface of the uterine glands (G) and endometrium (E), in granulosa cells (GC; b and c), in the extra-ovarian rete ovarii tubules (RO; d), in parts of the surface epithelium (OSE; b and c) and on

the surface of epithelial cells of the oviduct (ovi; e and f). Ciliated cells are indicated by an asterisk (*). Bars = 100 μm.

Figure 3.
OPCML immunohistochemistry in 4 µm sections of cystic ovaries from 9-month (b-c) and 12-month CD-1 mice (d-f) subjected to incessant ovulation from weaning. OPCML immunoreactivity was observed in the cells of normal and moderately dilated extra-ovarian rete ovarii (RO) tubules (a) and in the cells lining a cortical inclusion cyst with no connection to the ovarian hilus and therefore to the rete ovarii (b). Variable immunoreactivity was noted in flattened or ciliated cells (*) lining inclusion cysts with a hilar origin, most likely derived from dilation of the rete ovarii (c) - (f). The epithelium of papillary hilar inclusion cysts was weakly stained, especially on cells with a "signet ring" appearance (arrowhead) or when the cells contained lipid droplets (f). The granulosa cells

and zona pellucida of follicles were positively stained (foll). Bars in (a-c) and (e) = 100 μm and in (d) and (f) = 20 μm.

Table 1

Relative OPCML immunostaining in the cellular compartments of the oestrous mouse ovary. OPCML immunoreactivity was examined in stained 4 μm sections from 20 CD-1 mice (3 or 6 months, in oestrus) and graded 0-3 in intensity. Follicles showing disruption of the granulosa cell layers and evidence of pyknotic nuclei were classified as atretic. Results are expressed as the median and (range) of immunostaining intensity observed

Cellular compartment	Stain intensity
OSE	1 (0-3)
Granulosa cells in primordial or primary follicles	0 (0-0.5)
Oocytes/zona pellucida in primordial or primary follicles	1 (0.5-2)
Granulosa cells in healthy antral follicles	1 (1-3)
Oocytes/zona pellucida in healthy antral follicles	2 (1-3)
Granulosa cells in atretic antral follicles	2 (1-3)
Oocytes/zona pellucida in atretic antral follicles	1.5 (1-2)
Corpora lutea	1 (0-2)

Table 2

Mean ± SD of relative OPCML cDNA concentrations, normalised to ß-actin cDNA, in whole 3-month CD-1 mouse ovarian and uterine extracts at proestrus, oestrus and metoestrus or dioestrus, measured by qRT-PCR, calculated relative to a diluted uterine reference cDNA. Both gene sequences were amplified for each tissue extract in the same run. No significant differences in OPCML expression were observed with time of cycle

	OPCML/ß-actin	n
Ovary		
Proestrus	1.02 ± 0.52	5
Oestrus	1.37 ± 1.04	5
Met/dioestrus	1.32 ± 0.38	7
Uterus		
Proestrus	1.50 ± 0.53	5
Oestrus	1.62 ± 0.44	5
Met/dioestrus	2.22 ± 0.63	7